Advances in Bioceramics and porous ceramics II, Ceramic Engineering and Science Proceedings,
Vol. 30, Issue 6, pp. 179-190. R. Narayan & P. Colombo, Editors; D. Singh & J. Salem, Volume Editors. Wiley.

EFFECT OF ZINC ON BIOACTIVITY OF NANO-MACROPOROUS SODA-LIME PHOSPHOFLUOROSILICATE GLASS-CERAMIC

H.M. Moawad, S. Wang, H. Jain
Department of Materials Science & Engineering
Lehigh University, Bethlehem, PA 18015, USA

M. M. Falk
Department of Biological Sciences
Lehigh University, Bethlehem PA 18015, USA

ABSTRACT

Multi-scale porosity is desirable for the use of biocompatible glass and glass-ceramics as a bioscaffold material because porosity promotes cell attachment and thus better acceptance of the scaffolds. Recently, we demonstrated the fabrication of soda-lime phosphofluorosilicate glass-ceramics with porosity ranging from several nanometers to >100 micrometers by the melt-quench-heat-etch method, and optimized the phase distribution for rapid growth of hydroxyapatite (HA). In this work we have extended the usefulness of this class of biomaterial by adding ZnO that is believed to stimulate bone growth. Starting with $48SiO_2$-$2.7P_2O_5$-$4CaF_2$-xZnO-yCaO-zNa_2O glasses with x=0.0, 0.5, 1, 3, 5, 8, 10, y+z =45.3-x (mol %), nano-macro porous glass-ceramics were fabricated. We observed the formation of many crystalline phases, but mainly sodium calcium silicate, calcium phosphate, and fluorapatite. In general, the addition of ZnO improves glass durability. For $x \leq 3$ mol% HA is formed in simulated body fluid, but for higher concentration the surface layer deviates from HA composition significantly.

INTRODUCTION

Tissue engineering has been rapidly emerging as a viable option for the repair of skeletal tissues. One approach of tissue engineering considers the implantation of cells onto bioactive and degradable scaffolds that serve as temporary physical support.[1] Therefore, the design and construction of scaffold are attracting increasing attention for tissue engineering. An ideal bioscaffold should have the following characteristics: a) highly porous three-dimensional, interconnected pore network for cell growth and for the transport of nutrients and metabolic waste, b) biocompatible at all stages, c) bioresorbable with controlled degradation and resorption rate to match cell or tissue growth in vitro or in vivo, d) suitable surface chemistry for cell attachment, proliferation, and differentiation, and e) mechanical properties to match those of the tissues at the site of implantation.[2]

The pore fraction and structure are key parameters that determine the properties and applicability of scaffolds in a specific application. For glass as a candidate bone scaffold material, porosity is desired for cellular growth and attachment to the implant material's surface. It has been reported that bioactive glass forms a better bond with bone if it is porous.[2] There are advantages for nano-macroscale porosity, and the ideal bioactive glass should have this biomodal, even multi-modal porosity.[3,4] Irrespective of the size, it is important that the pores are interconnected for cell attachment, proliferation, differentiation, etc. Several methods have been developed in recent years for the fabrication of glass samples with these desired characteristics.[5-8] Here we focus on the melt-quench-heat-etch method developed in our laboratory recently, which is expected to yield samples of superior mechanical strength than those prepared by most other methods.[9,10] It is based on multi-scale spinodal phase separation, and therefore can be highly sensitive to the composition of glass.

Fluoride ions are usually added to drinking water and toothpastes, indicating their importance in bone repair or prevention of bone damage. In addition, the crystal structure of fluorapatite

($Ca_5(PO_4)_3F$) is very similar to the crystal structure of hydroxyapatite (HA), ($Ca_5(PO_4)_3(OH)$) that is the main inorganic mineral component of all bones. Therefore, recently we developed new soda lime phosphosilicate bioactive glass series doped with CaF_2 as a source of fluoride ions, and successfully introduced multi-modal interconnected porosity by the melt-quench-heat-etch method.[11] Our results indicated that there are four important parameters, which may affect the formation of HA layer on the surface of nano-macro porous soda-lime phosphofluorosilicate: initial glass composition, temperature of crystallization, type of crystalline phases and leached amount of useful $Na_2Ca_2Si_3O_9$ and $Ca_5(PO_4)_3F$ phases. As an example, Figure 1 shows remarkable effect of crystallization of the base glass of the present study on the compatibility of human MG63 osteoblast cells.[12] Note that the cells become rounded on the surface of untreated glass indicating not as good compatibility as with the partially crystallized glass-ceramic of the same overall composition where they stretch out and proliferate rapidly. The best results were obtained for our starting composition based on 48S glass series that contained 4-8 mol % CaF_2 and crystal growth temperature of 750°C.

It has been reported that incorporation of zinc into an implant material could promote bone formation around the implant and accelerate recovery of a patient.[13] Zinc is an essential trace element having stimulatory effects on bone formation in vitro and in vivo.[14] Therefore, in this work we have extended the usefulness of bioactive soda-lime phosphofluorosilicate based nano-macro porous scaffolds by doping the starting glass with ZnO as a source of zinc for the repair and reconstruction of hard tissues. Toward this goal, we have utilized X-ray diffraction, scanning electron microscopy and energy dispersive X-ray spectroscopy to identify the composition, phases and microstructures of our samples. In addition, mercury porosimeter and inductive coupling plasma methods were used to quantitatively characterize the pore size distribution and the effect of Zn content on the concentration of P, Ca and Si in simulated body fluid after the immersion of our porous glass-ceramic samples.

II. EXPERIMENTAL PROCEDURE

The glasses of composition $48SiO_2$-$2.7P_2O_5$-$4CaF_2$-$xZnO$-$yCaO$-zNa_2O; x=0.0, 0.5, 1, 3, 5, 8, 10, y+z =45.3-x (mol %) were prepared with SiO_2 (99.99%), $CaCO_3$ (99%), Na_2CO_3 (99%), $Ca_5(OH)(PO_4)_3$ (99%), CaF_2 (99%) and ZnO (99%) as starting materials. The calculated batch of powders was mixed and ground using an alumina mortar and pestle. It was melted in a platinum crucible at 1300°C for 2 hours. The homogenized melt was poured into a stainless steel mold and then the so formed glass was annealed at 500°C to relax residual stresses. The result was a glass phase-separated on nm scale with interconnected spinodal texture. To induce additional larger scale phase separation, the samples were subjected further to a devitrification heat treatment consisting of nucleation at 670°C for 1h, followed by crystal growth at 750°C for 6h. To create nano-macro porosity, the heat treated glasses were leached for 1 hour in 0.3N HCl at 85 °C. The glasses are identified such that the numbers preceding S, F and Z refer to the mol% of silica, calcium fluoride and zinc oxide, respectively. To indicate the transformation of a glass to glass-ceramic, letter G is added at the end. Thus, for example, 48S4F10ZG, represents a glass-ceramic made from glass containing 48 mol% SiO_2, 4 mol% CaF_2, 10 mol% ZnO.

To identify the phases and observe microstructure the samples were analyzed by X-ray diffraction (XRD) (Rigaku X-ray diffractometer) and scanning electron microscopy (SEM). Hitachi 4300 Field Emission SEM was used to examine sectioned and polished samples of each glass to elucidate the phase separation and microstructure. The elemental distribution in different phases was determined by energy dispersive X-ray (EDX) spectroscopy, using Cu K and Cu L as reference for peak position. The parameters for data acquisition (time, full scale for intensity, pulse processing time) were kept the same for all the samples. The pore size distribution of the samples was determined by mercury porosimeter (Micromeritics Auto pore IV).

The in vitro formation of apatite layer was observed in conventional simulated body fluid (SBF), where the fluid contained inorganic ions in concentration corresponding to human blood plasma. For the preparation of 1 liter of SBF, the following reagents were dissolved in distilled water in indicated amounts: 7.996g NaCl, 0.350g $NaHCO_3$, 0.224g KCl, 0.228g $K_2HPO_4.3H_2O$, 0.305g $MgCl_2.6H_2O$, 40ml 1N-HCl, 0.278g $CaCl_2$, 0.071g Na_2SO_4, 6.05g $NH_2C(CH_2OH)_3$.[4,15-17] The fluid was buffered at physiological pH of 7.4 at 37°C. Each glass or glass-ceramic specimen (2 mg) was immersed in 1 ml of SBF in a polyethylene bottle covered with a tight lid. The HA layer formed on the surface of the solid and porous glass-ceramic samples after soaking in SBF for 7 days was characterized by SEM, XRD, EDX and the solution was analyzed by the inductive coupling plasma (ICP) method (Perkin Elmer model 7300V ICP-OES).

III. RESULTS AND DISCUSSION

Figure 2 shows the microstructure of 48S4FG, 48S4F1ZG, 48S4F3ZG, 48S4F10ZG samples after the heat treatment. The micrographs of heat treated 48S4FxZG samples indicate that there are many crystalline phases. The XRD patterns of the 48S4F1ZG and 48S4F10ZG compositions are shown in Figure 3 as examples of our glass-ceramics. The location of most diffraction peaks matches the standard ICDD (International Center for Diffraction Data) powder diffraction file card numbers 15-177, 1-1078, 12-671 and 4-7-5856.[16-21]Accordingly, four distinct crystal phases are identified: $Ca_4P_6O_{19}$, $Na_2Ca_2Si_3O_9$, $Na_2CaSi_3O_8$, and $Ca_5(PO_4)_3F$. At the same time, there remain a few unidentified peaks indicating the presence of at least one new phase yet to be determined. None of the identified phases in 48S4FxZG appeared to be zinc compounds.

Figure 4 shows the development of porous structure with increasing zinc content when the heat treated samples of the 48S4FxZG (x= 1, 3, 8, 10 mol%) glass-ceramic series are subjected to chemical etching in 0.3N HCl at 85°C for 1h. The inset in Fig. 3(c) shows the microstructure of 48S4F3ZG sample at a much higher magnification, where nanoscale pores can be seen readily. It is clear from the micrographs in Fig. 4 (c), obtained at relatively low and high magnifications, that the present melt-quench-heat-etch method has produced a structured network of interconnected nano-macro porosity. The nano-macro interconnected porosity in our glass-ceramic samples has been confirmed by mercury porosimeter. In Fig. 5 we show an example of multi-modal nano-macro porosity in the present glass-ceramic series. The mechanism for the creation of multi-modal nano-macro interconnected porosity in these samples appears to be similar to that observed in zinc-free composition investigated previously.[9] It is observed from a comparison of micrographs of 48S4FxZG glass-ceramic samples in Fig. 3 that the macropore density decreases with increasing ZnO content from 1 to 10 mol%.

Figure 6 shows SEM micrographs of the 48S4FxZG series of glass-ceramics (for x=0, 0.5, 3, 8 and 10) after soaking in SBF for 7 days. Note that a layer is formed on the surface of all the samples. Presumably, the so formed layer is HA enriched with Ca and P. It covers the whole surface of our porous samples. Note that the deposited large particles aggregate on the surface of 48S4FxZG samples with x =0-3 mol% ZnO. By comparison, there are smaller particles aggregated on the surface of samples containing x = 8 and 10 mol% ZnO.

The composition of the layer formed on the surface of glass-ceramic samples is determined by EDX. Figure 7 shows selected examples of EDX spectra for the surface layer on various nano-macro porous glass-ceramic samples with x = 0, 3, 8 mol% ZnO. We note that the intensity of two key elements, Ca and P, decreases with increasing ZnO. It is known that $Na_2Ca_2Si_3O_9$ and $Na_2CaSi_3O_8$ strongly enhance the bioactivity of glass-ceramics.[8,19]At the same time, the crystal structure of crystalline $Ca_5(PO_4)_3F$ (fluorapatite) is very similar to the structure of HA.[22] Thus, fluorapatite crystalline phase acts as a seed or nucleation center for the formation of HA phase. Following our previous work,[11] we propose that it is predominantly the existence of $Na_2Ca_2Si_3O_9$ and $Ca_5(PO_4)_3F$ that causes the enhancement of HA formation on the surface of 48S4FxZG porous glass-ceramic samples.

On the other hand, it seems that the addition of more than 3 mol% ZnO decreases apatite forming ability on the surface of the samples.

Figure 8 shows changes in the elemental concentration of SBF after soaking of the porous glass-ceramic 48S4FxZG series for 1 to 5 days. Here we note the effect of soaking time and the concentration of ZnO in starting glass on the leaching of ions into SBF. Specifically, the phosphorus concentration decreases with increasing soaking time for porous glass-ceramics containing 0 to 1 mol% ZnO. On the contrary, it increases with increasing time in the range of composition with x=5 to 10 mol% ZnO. For the sample made with x=3 mol% ZnO glass, P concentration decreases with time, but its magnitude is significantly higher than that for x=0-1.

A similar leaching trend is observed for calcium whose concentration decreases with increasing time for x=0-3 mol% ZnO. Again as for phosphorous, its concentration in solution increases with time for x=5-10 mol% ZnO. We believe that the decrease in phosphorous and calcium concentration is due to the consumption of phosphate and calcium ions needed for the formation of apatite on the surface of samples with x=0-3 mol% ZnO. In contrast to P and Ca, the concentration of silicon in solution increases with the soaking time, but decreases with increasing x for the whole 0-10 mol% ZnO composition range. The increase in silicon with soaking time in the SBF solution indicates the release of silicate ions from the dissolution of samples. Evidently, the release of phosphorous, calcium and silicon from porous glass-ceramic samples is significantly affected by the concentration of ZnO in the starting glass.

To understand the effect of zinc oxide addition on apatite formation on the surface of these novel porous glass-ceramics, one should consider the reaction between the samples and SBF. The reaction of Si-Na-K-Ca-Mg-P-O glasses with SBF has been described by Hench.[23] Briefly, it takes place in following steps: (a) The exchange of Na^+ and K^+ from the glass with H^+ or H_3O^+ in SBF. This ion exchange is accompanied by the loss of silica into the solution and the formation of silanol on the glass surface. This step is followed by the condensation and polymerization of a SiO_2-rich layer on the surface. (b) Migration of Ca^{2+} and PO^{3-}_4 through the silica-rich layer forming a CaO-P_2O_5-rich film that also incorporates calcium and phosphate from SBF. (c) The final step is the crystallization of the amorphous calcium phosphate film to form an apatite layer. Preliminary results show that the glass-ceramic dissolution rate decreases with increasing ZnO, especially for x >3 mol%. Any of these steps can impact the dissolution process, and it is difficult to establish the rate determining step from the present data. The improvement in durability and apatite forming ability shows opposite dependence on ZnO content. Thus, it is very important to balance the two factors in optimizing the composition of present nano-macro porous glass-ceramics.

IV. CONCLUSION

Nano-macro porous glass-ceramics containing $Ca_4P_6O_{19}$, $Na_2Ca_2Si_3O_9$, $Na_2CaSi_3O_8$ and $Ca_5(PO_4)_3F$ crystalline phases were fabricated starting from soda-lime phosphofluorosilicate glasses doped with 0-10 mol% ZnO. The HA forming ability on the surface of porous glass-ceramic samples and hence bioactivity is significantly influenced by the mol % of ZnO in the initial glass and consequently the crystalline phases remaining in the samples after the chemical treatment. Specifically, the formation of HA remains unaffected by the addition of up to 3 mol% ZnO, but deteriorates for higher ZnO content. On the other hand, the chemical durability exhibits an inverse trend such that the glass-ceramic becomes significantly more durable for more than 3 mol% ZnO. Our processing parameters have been optimized with respect to the creation of multi-modal porosity and the formation of HA layer on 48S4FxZG (x=0-3 mol% ZnO) porous glass-ceramic.

ACKNOWLEDGEMENT

This work was initiated and continued as an international collaboration with support from National Science Foundation (International Materials Institute for New Functionality in Glass (DMR-0409588) and Materials World Network (DMR-0602975) programs). MMF is funded by the National Institutes of Health (NIH, NIGMS, grant GM55725). We thank Drs. Arup K. Sengupta and Sudipta Sarkar for help with the ICP measurements.

REFERENCES

[1]E.A. Abou Neel, I. Ahmed, J.J. Blaker, A. Bismarck, A.R. Boccaccini, M.P. Lewis, S.N. Nazhat and J.C. Knowles, *Acta Biomat.*, 1 553-563 (2005).
[2] A.R. Boccaccini and V. Maquet, *Compos. Sci. and Tech.,* 63 2417-2429 (2003).
[3] F. Balas, D. Arcos, J. Perez-Pariente and M. Vallet-Regi, *J. Mater. Res.*, 16 [5] 1345-8 (2001).
[4] P. Sepulveda, J.R. Jones and L.L. Hench, *J. Biomed. Mater. Res*., 59 [2] 340-348 (2002).
[5] A.C. Marques, H. Jain and R.M. Almeida, *Eur. J. Glass. Sci. Tech.* 48 65-68 (2007).
[6]N. Li, Q. Jie, S. Zhu and R. Wang, *Ceram. Internat*., 31 [5] 641-646 (2005).
[7] M.N. Rahaman, W. Liang and E. Day, *Ceram. Eng. Sci. Proceeding*, 26 [6] 3-10 (2005).
[8] T. Peltola, M. Jokinen, H. Rahiala, E. Levanen, J.B. Rosenholm, I. Kangasniemi and A. Yli-Urpo, *J. Biomed Mat. Res.*, 44 12-21 (1999).
[9] H.M.M. Moawad and H. Jain, *J. Am. Ceram. Soc.,* 90 [6] 1934-6 (2007).
[10] H.M.M. Moawad and H. Jain, *Ceram. Eng. Sci. Proc.,* Development in Porous, Biological and Geopolymer Ceramics, 28 [9] 183-195 (2008).
[11] H.M.M. Moawad and H. Jain, *J. Mater. Sci. Mater. Med.*, in press.
[12] A. Billiau, V.G. Edy, H. Heremans, J. Van Damme, J. Desmyter, J.A. Georgiades and P. De Somer, *Human interferon*, 12 11-25 (1977).
[13]A. Ito, K. Ojima, H. Naito, N. Ichinose and T. Tateishi, J. Biomed. Mat. Res., 50 178-183 (2000).
[14] A. Ito, H. Kawamura, M. Otsuka, H. Ikeuchi, H. Ohgushi, K. Ishikawa, K. Onuma, N. Kanzaki, Y. Sogo and N. Noboru, *Mat. Sci. Eng.,* C22 21-25 (2002).
[15] H.M. Kim, T. Miyazaki, T. Kokubo and T. Nakamura, *Key Eng. Mater.* 192-195 47-50 (2001).

[16] H.A. El-Batal, M. A. Azooz, E.M.A. Khalil, A.S. Monem and Y.M. Hamdy, *Mater. Chem. Phys.,* 80 599-609 (2003).
[17]S. Jalota, S.B. Bhaduri, A.C. Tas**,** *J. Mater. Sci. Mater. Med.,* 17 697-707 (2006).
[18] T.H. Elemer, M.E. Nordberg, G.B. Carrier and E.J. Korda, *J. Amer. Ceram. Soc.,* 53 171-175 (1970).
[19] O.P. Filho, G.P. LaTorre and L.L. Hench, *J. Biomed. Mater. Res.,* 30 509-514 (1996).
[20]O. Peitl, E.D. Zanotto and L.L. Hench, *J. Non-Cryst. Solids,* 292 115-126 (2001).
[21] X. Chen, L.L. Hench, D. Greespan, J. Zhong and X. Zhang, *Ceramic Internat.,* 24 401-410 (1998).
[22] M. Mathew and S. Takagi, *J. Res. Nat. Inst. Stand. Technol.* 106 1035-1044 (2001).
[23] L.L. Hench, *J. Am. Ceram. Soc.*, 74(4) 1487-1510 (1991).

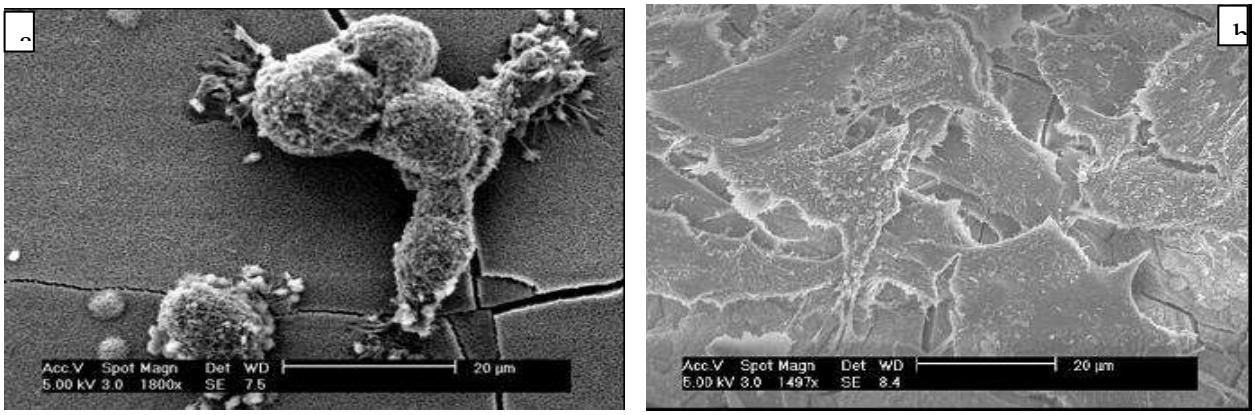

Figure 1. SEM picture of human MG63 osteoblast cells on the surface of $48SiO_2$-$2.7P_2O_5$-$4CaF_2$-$24.2CaO$-$21.1Na_2O$ (a) glass and (b) glass-ceramic of the same composition.

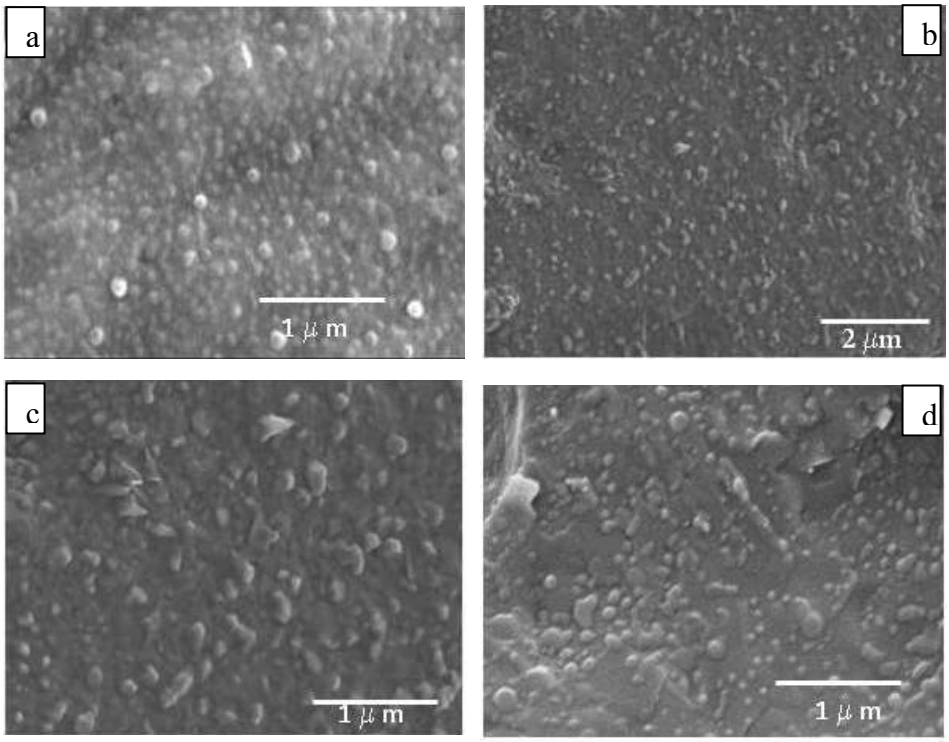

Figure 2: Low magnification SEM micrographs of 48S4FxZG specimens containing x mol% ZnO after the heat treatment: a) x=0, b) x=1, c) x=3, d) x=10.

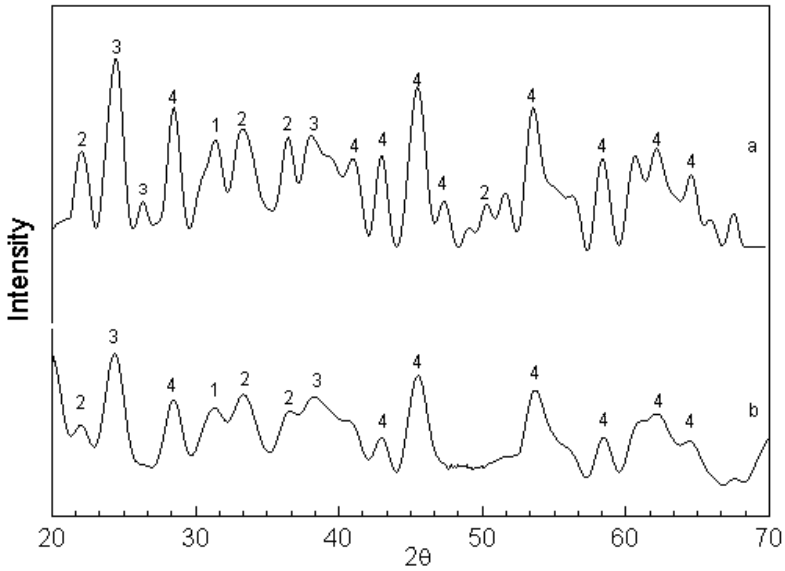

Figure 3: X-ray diffraction patterns of glass-ceramic samples after the nucleation and growth heat treatments: a) 48S4F1ZG, b) 48S4F10ZG, the source of diffraction peaks: 1) $Ca_4P_6O_{19}$, 2) $Na_2Ca_2Si_3O_9$, 3) $Na_2CaSi_3O_8$, 4) $Ca_5(PO_4)_3F$.

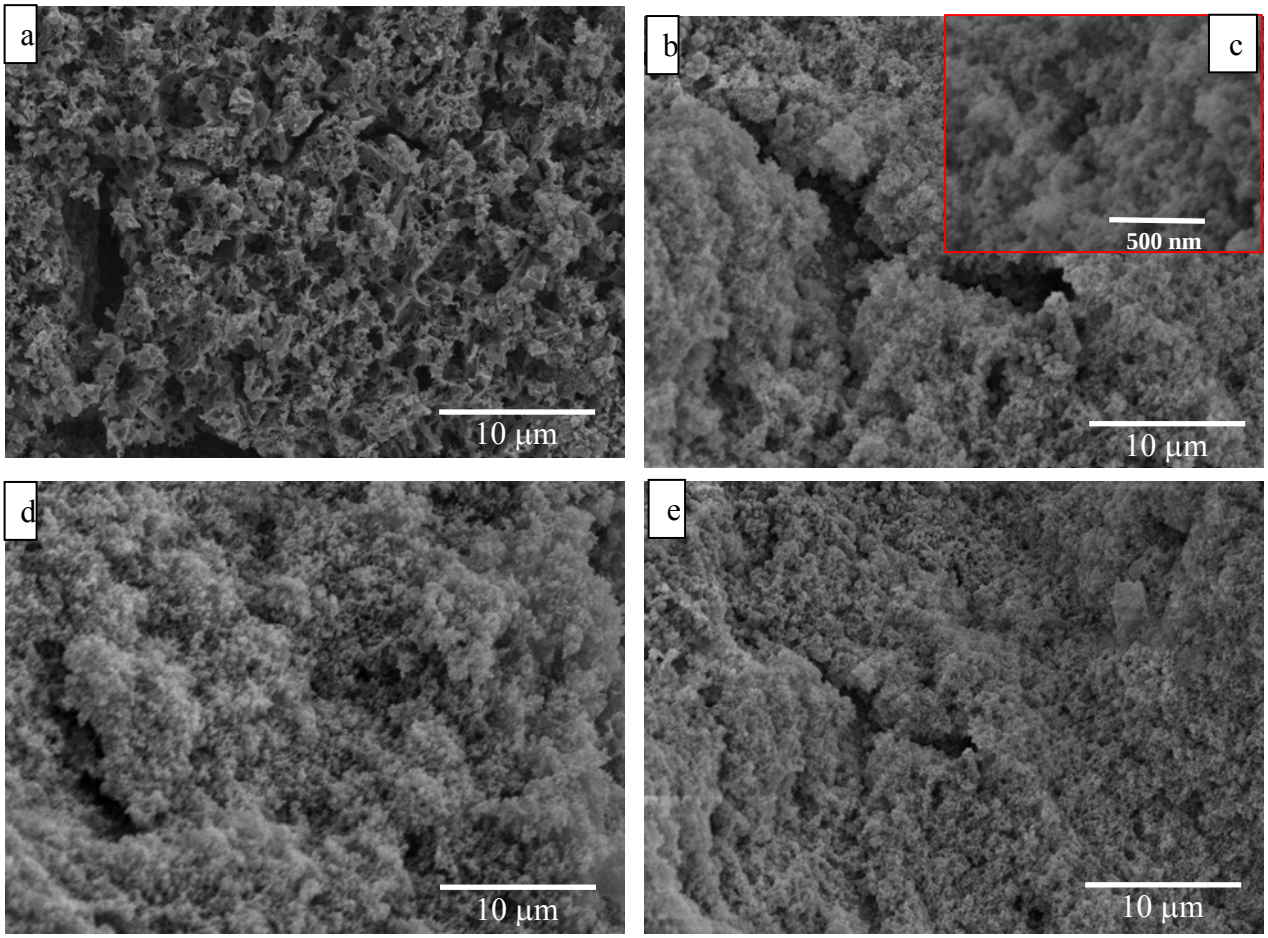

Figure 4: Low magnification SEM micrographs of 48S4FxZG specimens after heat treatment + chemical leaching: a) x=1 mol%, b, c) x=3 mol%, d) x=8 mol%, e) x=10 mol%. The inset (c) is a high magnification image of the sample (b).

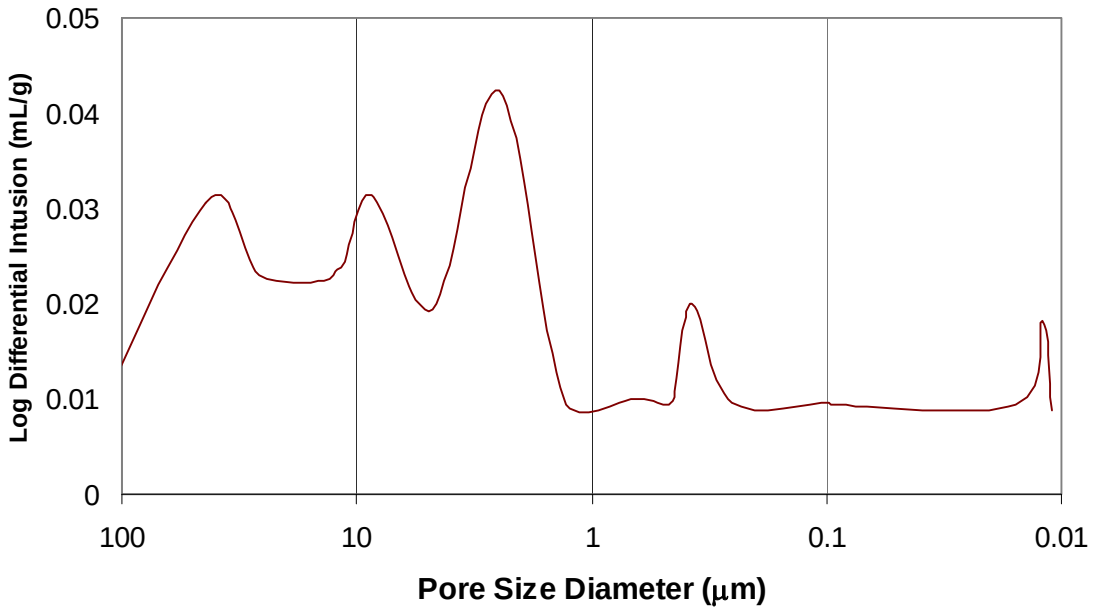

Figure 5: Mercury porosimeter data showing the distribution of pore size in 48S4F3ZG specimens after heat treatment + chemical leaching.

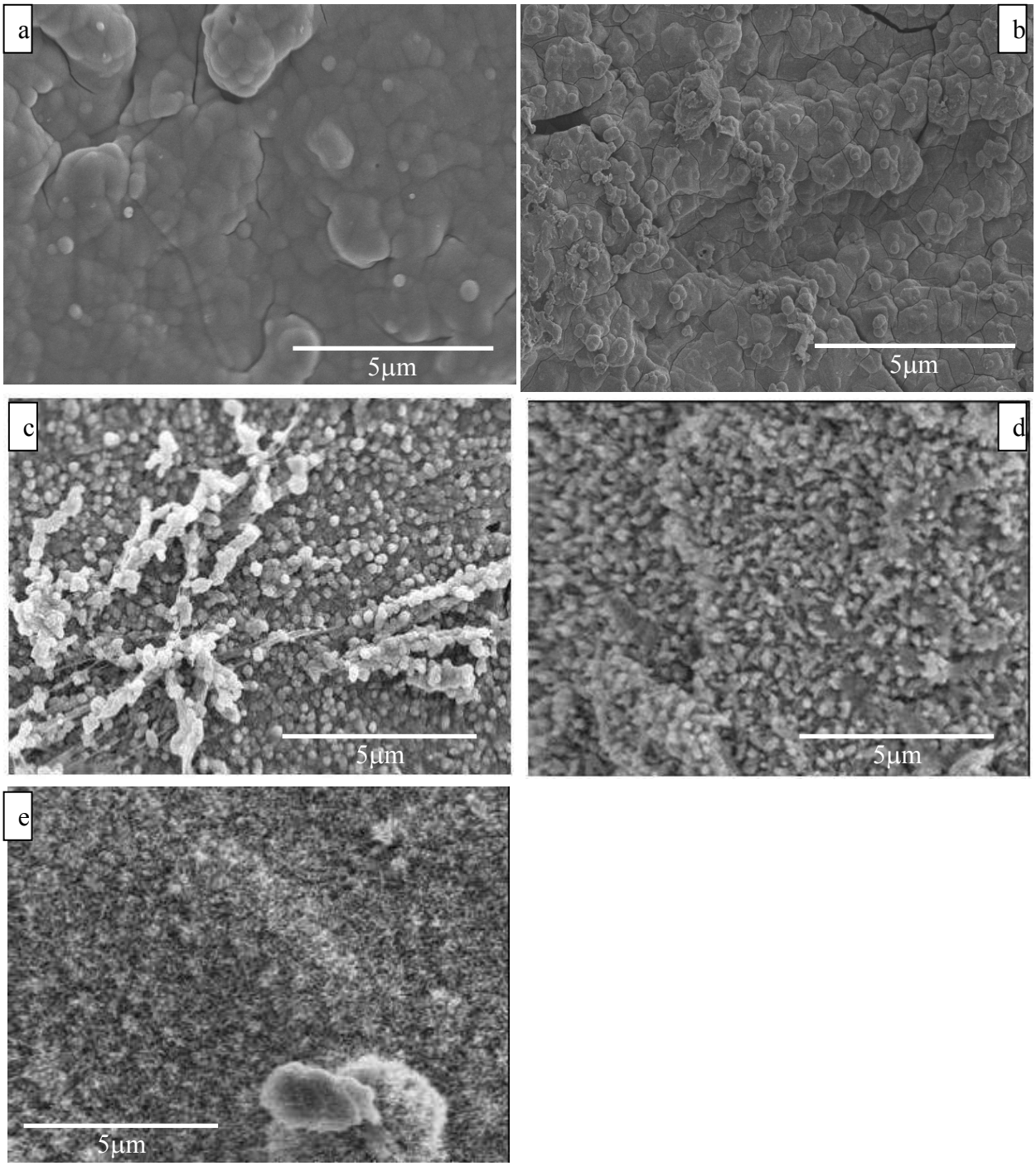

Figure 6: SEM micrographs of chemically treated glass-ceramic after soaking for 7 days in SBF: a) 8S4FG, b) 48S4F0.5ZG, c) 48S4F3ZG, d) 48S4F8ZG, e) 48S4F10ZG.

.

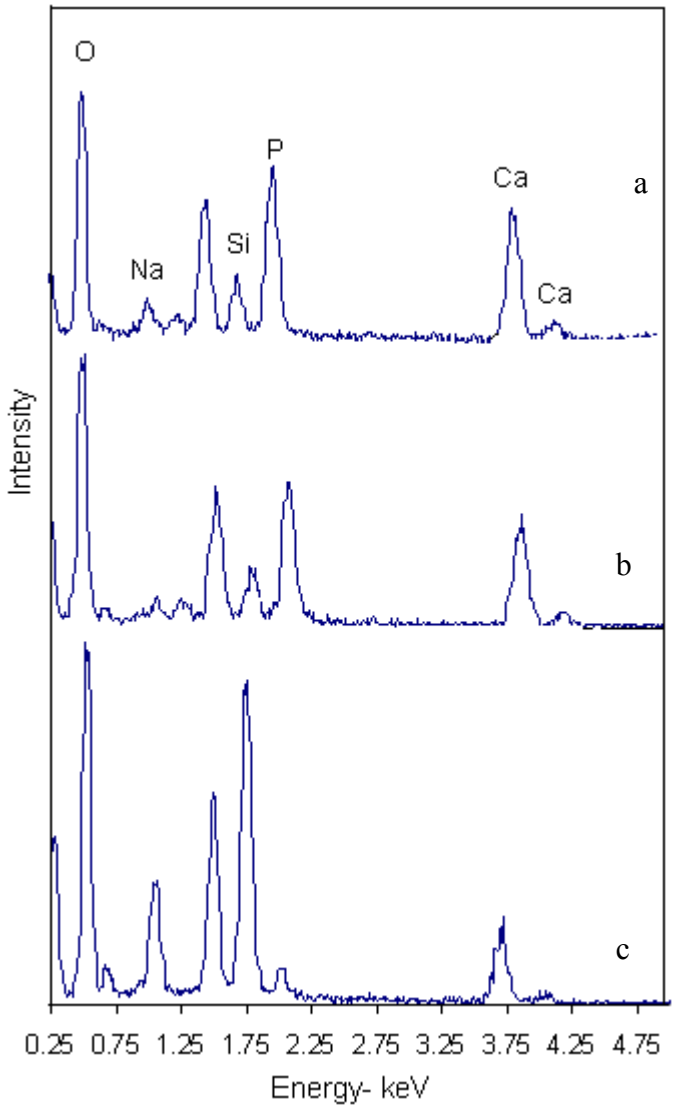

Figure 7: EDX spectra of chemically treated glass-ceramic after soaking for 7 days in SBF: a) 48S4FG, b) 48S4F3ZG, c) 48S4F8ZG. The peak at ~1.4 eV is from aluminum stub holding the sample.

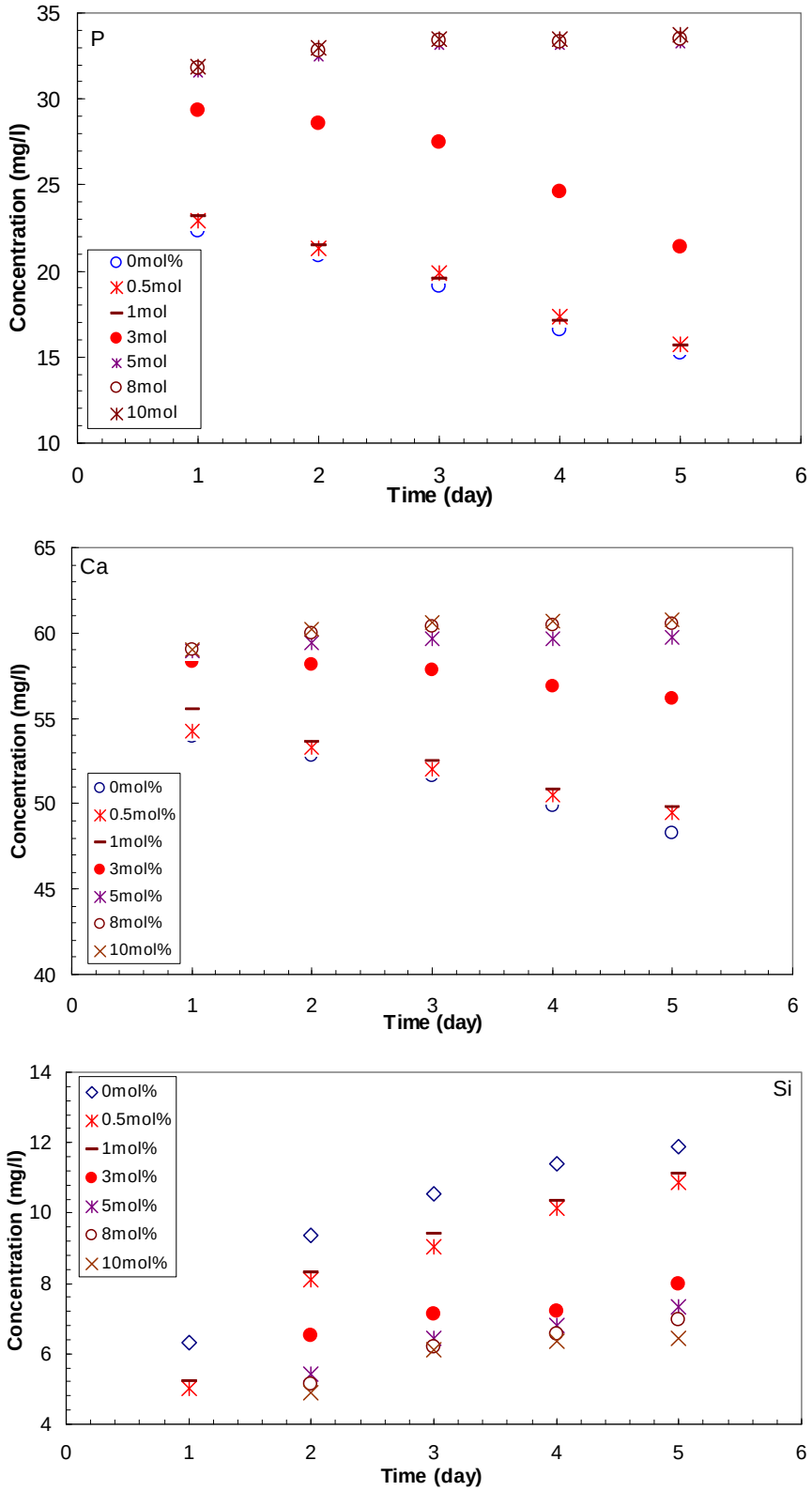

Figure 8: The change of P, Ca and Si concentration in SBF with immersion time of porous glass-ceramic 48S4FxZG with various ZnO content.